Mol Genet Genomics (2011) 285:341–354
DOI 10.1007/s00438-011-0611-6

ORIGINAL PAPER

Phylogenetic and genetic linkage between novel atypical dual-specificity phosphatases from non-metazoan organisms

Carlos Romá-Mateo · Almudena Sacristán-Reviriego · Nicola J. Beresford · José Antonio Caparrós-Martín · Francisco A. Culiáñez-Macià · Humberto Martín · María Molina · Lydia Tabernero · Rafael Pulido

Received: 6 August 2010 / Accepted: 27 February 2011 / Published online: 16 March 2011

Abstract Dual-specificity phosphatases (DSPs) constitute a large protein tyrosine phosphatase (PTP) family, with examples in distant evolutive phyla. PFA-DSPs (*P*lant and *F*ungi *A*typical DSPs) are a group of atypical DSPs present in plants, fungi, kinetoplastids, and slime molds, the members of which share structural similarity with atypical- and lipid phosphatase DSPs from mammals. The analysis of the PFA-DSPs from the plant *Arabidopsis thaliana* (AtPFA-DSPs) showed differential tissue mRNA expression, substrate specificity, and catalytic activity for these proteins, suggesting different functional roles among plant PFA-DSPs. Bioinformatic analysis revealed the existence of novel PFA-DSP-related proteins in fungi (Oca1, Oca2, Oca4 and Oca6 in *Saccharomyces cerevisiae*) and protozoa, which were segregated from plant PFA-DSPs. The closest yeast homolog for these proteins was the PFA-DSP from *S. cerevisiae* ScPFA-DSP1/Siw14/Oca3. Oca1, Oca2, Siw14/Oca3, Oca4, and Oca6 were involved in the yeast response to caffeine and rapamycin stresses. Siw14/Oca3 was an active phosphatase in vitro, whereas no phosphatase activity could be detected for Oca1. Remarkably, overexpression of Siw14/Oca3 suppressed the caffeine sensitivity of *oca1*, *oca2*, *oca4*, and *oca6* deleted strains, indicating a genetic linkage and suggesting a

Communicated by M. Collart.

Electronic supplementary material The online version of this article (doi:10.1007/s00438-011-0611-6) contains supplementary material, which is available to authorized users.

C. Romá-Mateo · R. Pulido (✉)
Centro de Investigación Príncipe Felipe,
Avenida Autopista del Saler 16-3, 46013 Valencia, Spain
e-mail: rpulido@cipf.es

C. Romá-Mateo
e-mail: croma@ibv.csic.es

A. Sacristán-Reviriego · H. Martín · M. Molina
Facultad de Farmacia, Universidad Complutense
de Madrid, 28040 Madrid, Spain
e-mail: jarmuilla3@hotmail.com

H. Martín
e-mail: humberto@farm.ucm.es

M. Molina
e-mail: molmifa@farm.ucm.es

N. J. Beresford · L. Tabernero
Faculty of Life Sciences, Michael Smith Building,
University of Manchester, Manchester M13 9PT, UK
e-mail: nberesf@nimr.mrc.ac.uk

L. Tabernero
e-mail: lydia.tabernero@manchester.ac.uk

J. A. Caparrós-Martín · F. A. Culiáñez-Macià
Instituto de Biologia Molecular y Celular de Plantas
Primo-Yúfera, Universidad Politécnica de Valencia-CSIC,
Avenida de los Naranjos s/n, 46022 Valencia, Spain
e-mail: jacapmar@gmail.com

F. A. Culiáñez-Macià
e-mail: faculia@ibmcp.upv.es

Present Address:
C. Romá-Mateo
Instituto de Biomedicina de Valencia, CSIC and Centro de
Investigación Biomédica en Red de Enfermedades Raras
(CIBERER), Jaime Roig 11, 46010 Valencia, Spain

Present Address:
N. J. Beresford
Mycobacterial Research, National Institute for Medical Research
the Ridgeway, Mill Hill, London NW7 1AA, UK

functional relationship for these proteins. Functional studies on mutations targeting putative catalytic residues from the *A. thaliana* AtPFA-DSP1/At1g05000 protein indicated the absence of canonical amino acids acting as the general acid/base in the phosphor-ester hydrolysis, which suggests a specific mechanism of reaction for PFA-DSPs and related enzymes. Our studies demonstrate the existence of novel phosphatase protein families in fungi and protozoa, with active and inactive enzymes linked in common signaling pathways. This illustrates the catalytic and functional complexity of the expanding family of atypical dual-specificity phosphatases in non-metazoans, including parasite organisms responsible for infectious human diseases.

Keywords Phosphatase · Phosphorylation

Introduction

The protein tyrosine phosphatase (PTP) superfamily constitutes a large group of enzymes, evolutionarily related, with a conserved catalytic PTP domain and a common Cys-based mechanism of catalysis (Alonso et al. 2004a). Although in higher metazoans, such as mammals, the complete repertoire of PTPs and their basic functional properties are well established, the knowledge of the PTP members from evolutionarily distant organisms is less complete. Comprehensive studies on the existence of PTPs in organisms from different phyla have revealed that the dual-specificity phosphatase (DSP) subfamily of PTPs is the one more widely represented, with examples in all the life kingdoms (Kennelly 2001; Brenchley et al. 2007; Pincus et al. 2008; Moorhead et al. 2009). In mammals, more than 60 distinct DSPs exist, clustered in subfamilies that show a relatively high degree of structural and functional diversity, including monomeric and oligomeric enzymes that dephosphorylate a wide variety of protein-, lipid-, RNA-, and carbohydrate-substrates. Major subfamilies of mammalian DSPs include: the MKP (MAP kinase phosphatase) family, the members of which display specificity toward MAP kinases; the MKP-like low molecular weight atypical DSP family (DUSP3/VHR being the prototype); and the lipid-phosphatase families represented by myotubularins, PTEN, and PTEN-related proteins (Maehama et al. 2001; Alonso et al. 2004b; Owens and Keyse 2007). Interestingly, both the classical PTP and DSP subfamilies contain inactive enzymes, the functions of which have been proposed to be related to the regulation of active PTPs (Wishart and Dixon 1998). The functional properties and the physiological roles of DSPs in organisms from non-metazoan kingdoms have been scarcely studied. In fungi and plants, MKP-like DSPs have been identified that are involved in the dephosphorylation and inactivation of MAP kinases in these organisms (Luan 2003; Martin et al. 2005). The *Arabidopsis thaliana* AtMKP1 is involved in the defense to genotoxic stress, including abiotic and salinity stresses (Ulm et al. 2001, 2002; Bartels et al. 2009). In the yeast *Saccharomyces cerevisiae*, the MKP-like Msg5 and Sdp1 are key regulators of the pheromone and the cell wall integrity-pathways (Doi et al. 1994; Hahn and Thiele 2002; Flandez et al. 2004). Interestingly, Msg5 and Sdp1 have been proposed to belong to a unique group of fungal phosphatases, on the basis of substrate recognition mediated by oxidation (Fox et al. 2007). MKP-like DSP sequences are also present in kinetoplastid and Apicomplexa parasites, such as species of *Trypanosoma*, *Leishmania*, and *Plasmodium*, which cause severe human diseases. Also, DSPs with predicted protein- and lipid-phosphatase activity have been found in these phyla and in bacteria, although their physiological substrates remain uncertain in most of the cases (Brenchley et al. 2007; Andreeva and Kutuzov 2008; Wilkes and Doerig 2008; Beresford et al. 2010). Using bioinformatics, modeling analysis, and biochemical tools, we have defined a novel family of DSPs with members belonging to species of plants, fungi, kinetoplastids, and slime molds (PFA-DSPs) (Romá-Mateo et al. 2007). PFA-DSPs share the presence of four common amino acid motifs (PF1–PF4 fingerprint motifs; average side, 16 residues), which segregates this family from other DSP families (Attwood and Findlay 1993; Nordle et al. 2007) (http://www.bioinf.manchester.ac.uk/dbbrowser/PRINTS/index.php). The catalytic domains of PFA-DSPs do not have significant homology at the amino acid level with DSP catalytic domains from animals (with the exception of the signature catalytic motif), but the three-dimensional folding of the PFA-DSP AtPFA-DSP1/At1g05000 resembles that of mammalian DSPs (Aceti et al. 2008). The *A. thaliana* AtPFA-DSP1, -2, and -3 are active phosphatases in vitro, and AtPFA-DSP1 does not complement the activity of the mammalian DUSP3/VHR or PTEN (Romá-Mateo et al. 2007) (and our unpublished results), suggesting specific physiological functions for the AtPFA-DSP proteins. On the other hand, there are no published data on the physiological function of PFA-DSPs, with the exception of the PFA-DSP from the yeast *S. cerevisiae*, Siw14/Oca3, which has been reported to control cell cycle arrest in response to nutrient deprivation, as well as the intracellular location of the transcriptional activator Gln3 (Care et al. 2004; Hirasaki et al. 2008). Oca1, which is identified in the present study as a yeast PFA-DSP-related protein, has also been involved in the cell cycle arrest response to oxidative stress (Alic et al. 2001). Here, we report the existence of novel PFA-DSP-related proteins in fungi and protozoa. Our results indicate that PFA-DSPs and related proteins have wider species distribution than previously described, and provide insights into the gene expression patterns,

catalytic mechanism, and genetic linkages of these proteins in non-metazoan organisms.

Methods

Bioinformatics

Sequences were obtained by BLASTP searches using AtPFA-DSP1, Siw14/Oca3, TbPFA-DSP1, and DdPFA-DSP1, and limiting the search to *Viridiplantae*, *Fungi*, and *Protozoa* taxa in NCBI databases. A second round of BLASTP searches was performed using the sequences of Oca1, Oca2, and Oca6 from *S. cerevisiae* in the same taxa. Finally, a third round of searches was performed with all the set of sequences in metazoan organisms, not finding significant similarities (*e* value limit $= 1 \times 10^{-13}$ for all BLASTP searches). All the sequences obtained by the different searches were aligned using CLUSTALX and those not containing the catalytic consensus site for DSPs were removed from the alignment, with the exception of Oca4 from *S. cerevisiae*. This multiple alignment was edited to contain only the catalytic domain of the proteins, and a maximum-likelihood phylogenetic tree with 100 bootstrap replicates was created using PhyML software (Guindon and Gascuel 2003). A consensus dendrogram was calculated using Phylip package (Felsentein 1989), and the final tree was visualized using TreeView software (Page 1996). Structural models were created using the structure of AtPFA-DSP1 (PDB:1xri) as a template and the Esypred3D on-line server (Lambert et al. 2002). The models were visualized using PyMOL (http://www.pymol.org) and images were created with a PyMOL plug-in that utilizes the APBS electrostatic surface evaluation tool (Baker et al. 2001).

Semi-quantitative and quantitative real-time PCR analysis

Total RNA samples from root, stem, leaf, flower, and silique were purified from *A. thaliana* adult plants using TriReagent and GenElute for Mammalian total RNA kit (Sigma). For semi-quantitative PCR analysis, in which the amount of final PCR product is measured, 10 ng of total RNA was used as the template in one-step RT-PCR reactions using Titan One tube RTPCR System (Roche). For quantitative real-time PCR, 1–1.5 μg of total RNA was used in RT reactions using commercial RevertAid H Minus M-MuLV Reverse transcriptase (Fermentas). As much as 100 ng of each resulting cDNA was used as the template in qRT-PCR reactions with specific primers designed using Probe Design Software 2.0 (*Roche*) (with efficiencies ranging from 1.9 to 2.2). Reactions were carried out in Roche LightCycler 480 Real-Time PCR System using SYBR green dye. Ct values obtained for each gene were normalized (Pfaffl 2001) using AtPFA-DSP2 expression, and relative abundance of AtPFA-DSP mRNAs in each tissue was calculated (100%, maximum value). The sequences of the primers are available upon request.

Plasmids and mutagenesis

pGEX-4T-AtPFA-DSP1, -2, and -3 (encoding the corresponding GST-fusion proteins) have been described (Romá-Mateo et al. 2007). pYES2-AtPFA-DSP1 was obtained by subcloning from pGEX-4T-AtPFA-DSP1. pGEX-4T-AtPFA-DSP5 was obtained by PCR subcloning from pUni51-At5g16480 (ABRC DNA Stock Center). pGEX-4T-Siw14 and pGEX-4T-Oca1 were obtained by PCR subcloning from pYES-Siw14 (provided by P. Sudbery, The University of Sheffield, UK) and pYCG-Oca1p (provided by J.L. Revuelta, Universidad de Salamanca, Spain), respectively. The different yeast *OCA* genes were overexpressed under the control of the *GAL1* promoter, from the corresponding plasmids based on the vector BG1805 (C-terminal tags: poly-His, hemagglutinin, and protein A) obtained from Open-Biosystems. AtPFA-DSP1 was overexpressed from the same promoter by using plasmid pYES2-AtPFA-DSP1 (no tagging). pYES2 (Invitrogen) was used as a control empty vector. Mutations were made by PCR oligonucleotide site-directed mutagenesis. All constructs and mutations were confirmed by DNA sequencing.

In vitro phosphatase assays

Recombinant GST-fusion proteins containing the full-length phosphatases were affinity purified from *E. coli* using gluthatione-Sepharose beads and dialyzed in the appropriate phosphatase reaction buffer. For pNPP hydrolysis, purified proteins were incubated with pNPP (10 mM, Sigma) in 0.1 M Tris–HCl of pH 8.0, 40 mM NaCl and 10 mM DTT (reaction buffer A) for 90 min at 37°C, followed by measurement of absorbance at 405 nm. For OMFP hydrolysis, purified proteins were incubated with OMFP (0.5 mM, Sigma) in reaction buffer A, followed by measurement of absorbance at 490 nm. To determine the kinetic parameters for pNPP, the initial velocities were measured at different pNPP concentrations ranging from 0.1 to 60 mM, and the data were fitted to the Michaelis–Menten equations by nonlinear regression and the program GraphPad Prism (http://www.graphpad.com). The hydrolysis of pTyr (5 mM, Sigma), and water-soluble diC_8-PI(3,5)P2 and diC8-PI(3,4,5)P3 (100 μM, Echelon) was performed in 0.1 M Tris–HCl of pH 8.0 and 10 mM DTT (reaction buffer B). The phosphate released was measured

by absorbance at 580/620 nm by the malachite green system (Sigma). Absorbance was measured in a WALLAC 1420 multiplate reader (PerkinElmer).

Yeast growth assays

The following isogenic yeast strains were used: *S. cerevisiae* BY4741 (*MATa*; *his3Δ1*; *leu2Δ0*; *lys2Δ0*; *ura3Δ0*), Y03702 (*ptc1/YDL006WΔ::kanMX4*) Y07235 (*oca1/YNL099cΔ::kanMX4*), Y07211 (*oca2/YNL056wΔ::kanMX4*), Y05358 (*siw14/oca3/YNL032wΔ::kanMX4*), Y06962 (*oca4/YCR095cΔ::kanMX4*), Y04002 (*oca6/YDR067cΔ::kanMX4*) (EUROSCARF, Frankfurt, Alemania). Yeast cells were grown during 16 h at 30°C in YPD (complete glucose-based medium) and then diluted to an OD_{600} value of 0.150. Five microliters of serial 1/10 dilutions was plated onto YPD and incubated for 3 days, in the absence or in the presence of the indicated concentrations of caffeine or rapamycin (Sigma). Yeast transformants were assayed as above except that they were grown in SD-Ura$^-$ medium and plated onto both YPD and YPG (complete galactose-based medium).

Results

PFA-DSP-related proteins from non-metazoan organisms

PFA-DSPs are present in species of plants, fungi, kinetoplastids, and slime molds, and are absent in mammals or any other metazoan organisms. Interestingly, plants are the only group of multicellular organisms in which PFA-DSPs are present. However, a comprehensive analysis of the presence and functional role of proteins related to PFA-DSPs on these and other taxa is lacking. To analyze the existence and species distribution of PFA-DSP and PFA-DSP-related sequences (as indicated by amino acid sequence similarity), we performed a series of BLASTP searches using the five *A. thaliana* proteins and each one of the yeast, kinetoplastid and *Dyctiostelium* orthologs as queries. The first round of searches returned, as expected, many other plant and yeast sequences together with several protozoan sequences. We repeated the searches limiting the BLASTs to taxon-specific databases; in this way, we found that many sequences appearing in the fungal genomes, although showing high scores with the query sequences and possessing the consensus catalytic site for DSPs, were not positive for the fingerprint PFA-DSP-motifs (only one or two motifs, out of the four fingerprint motifs, were present, and none of them produced the required *e* value of 0.0001 for being considered as a positive hit), as previously defined (Romá-Mateo et al. 2007). Fingerprint technology is a bioinformatic tool for defining very closely related protein families, which are grouped together by the presence of a set of conserved motifs (Attwood and Findlay 1994). Sequences with similarity, but which lack more than one of the motifs, are hence named as family-related proteins. Thus, we identified a series of amino acid sequences in yeast, related with the PFA-DSPs by sequence similarity, which had been annotated as Ocas in the yeast *S. cerevisiae* [Oca1, Oca2, and Oca6; note that Siw14/Oca3 was named as ScPFA-DSP1 in our former study (Romá-Mateo et al. 2007)], as well as a group of sequences (named here as Oca-like sequences) that were present in Euascomycota species, but not in *S. cerevisiae*. Next, we used the *S. cerevisiae* Oca1, Oca2, and Oca6 sequences to perform new BLAST searches and repeated this process until reciprocally finding the PFA-DSP sequences used in the first round, as indicated. The complete set of sequences resulting from all searches was then used for a multiple sequence alignment that permitted deletion of sequences not containing the consensus catalytic site for DSPs. Oca4 protein and orthologs, although lacking the consensus catalytic motif, were included in the final set of sequences due to their putative functional relation with the rest of Oca proteins (see below). The final set of sequences was then used as the seed for a maximum likelihood tree. As a result of this analysis, more precise orthologies were established between PFA-DSPs and PFA-DSP-related sequences in the distinct taxa, and plant PFA-DSPs were clustered together (Fig. 1). The same alignment was used for creation of a neighbor-joining tree, obtaining the same topology and similar bootstrap values (not shown). PFA-DSPs from plants and Siw14/Oca3 proteins from fungi and protozoa grouped close in the tree, confirming their previous definition as PFA-DSPs. The clade of Oca-like sequences, not represented in *S. cerevisiae*, was separated from the rest. Nodes including the PFA-DSP-related Oca proteins display a high bootstrap support, indicating that the sequences from protozoa that cluster with them represent putative orthologs. Remarkably, most of these sequences had not been previously reported, the majority of them belonging to protozoan species from the infrakingdom Excavata [including parasite organisms from phylum Euglenozoa (kinetoplastids from genera *Trypanosoma* and

Fig. 1 Phylogenetic dendrogram of PFA-DSPs and related proteins. ▶ Maximum likelihood tree showing phylogenetic relationships between PFA-DSP and PFA-DSP-related proteins (*left*). PFA-DSPs are represented as an outgroup (*colored triangles*; plants, *green*; fungi, *blue*; protozoan organisms, *red*). *Boxes* mark high bootstrap values (*black*, higher than 70; *white*, higher than 50). *Arrows* mark the situation of *S. cerevisiae* Oca proteins. On the *right side* a detailed expanded tree of PFA-DSPs is shown. Plants, *green*; fungi, *blue*; protozoan organisms, *red*. Only bootstrap values for the most relevant clusters of sequences are shown. Proteins are denoted by UniProt accession numbers

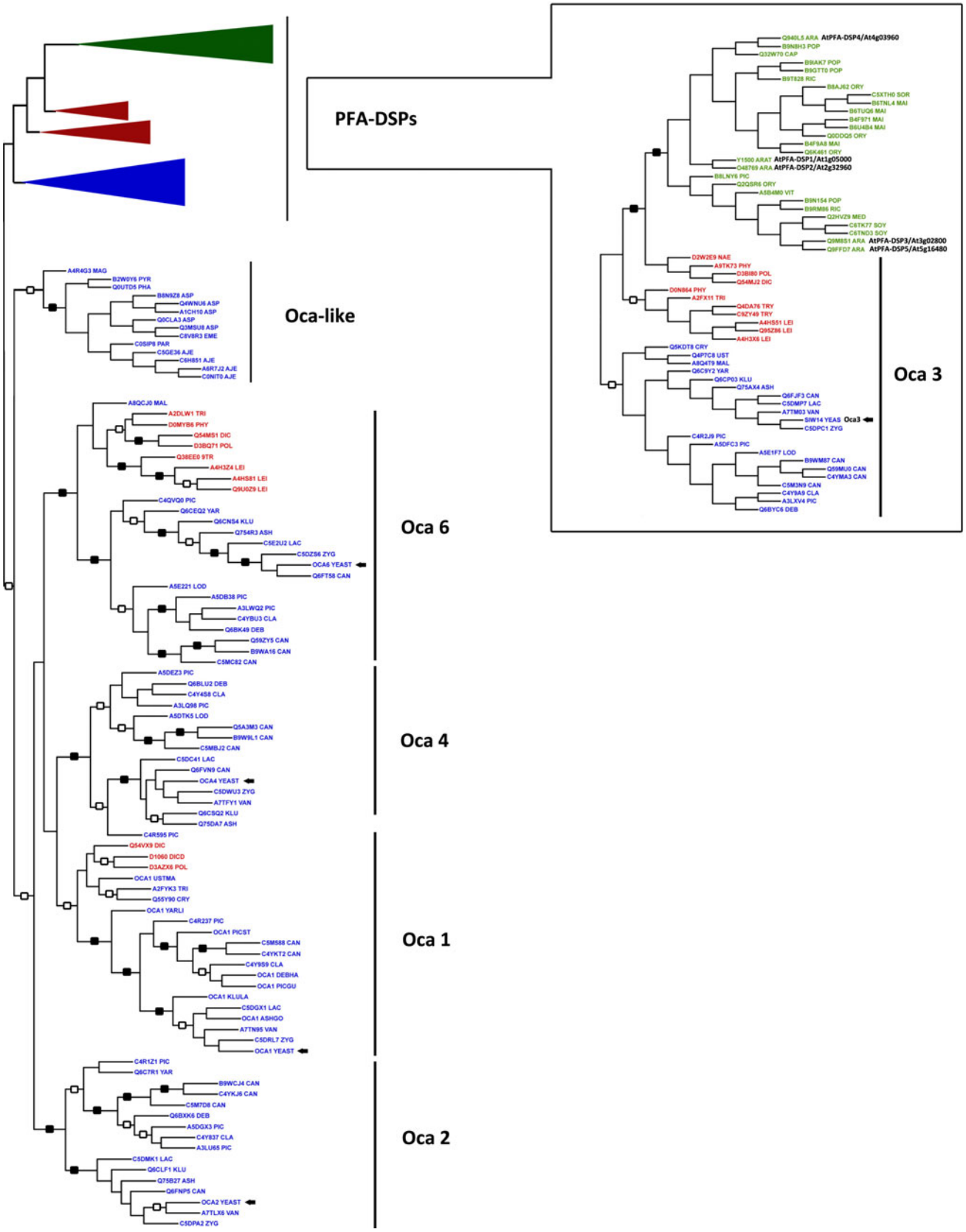
PFA-DSPs
Q940L5 ARA AtPFA-DSP4/At4g03960
B9N8H3 POP
Q32W70 CAP
B9AK7 POP
B9QTT0 POP
B9T828 RIC
B8AJ62 ORY
C5XTH0 SOR
B6TNL4 MAI
B6TUQ6 MAI
B4F971 MAI
B6U4B4 MAI
Q0DDQ5 ORY
B4F9A8 MAI
Q6K461 ORY
Y1500 ARAT AtPFA-DSP1/At1g05000
Q48769 ARA AtPFA-DSP2/At2g32960
B8LNY6 PIC
Q2QSR6 ORY
A5B4M0 VIT
B9N154 POP
B9RM86 RIC
Q2HVZ9 MED
C6TKT7 SOY
C6TND3 SOY
Q9M851 ARA AtPFA-DSP3/At3g02800
Q8FFD7 ARA AtPFA-DSP5/At5g16480
D2W2E9 NAE
A9TK73 PHY
D3BI80 POL
Q54MJ2 DIC
D0N864 PHY
A2FX11 TRI
Q4DA76 TRY
C8ZY49 TRY
A4HS51 LEI
Q95Z86 LEI
A4H3X6 LEI
Q5KDT8 CRY
Q4P7C8 UST
A8Q4T9 MAL
Q6C9Y2 YAR
Q6CP03 KLU
Q75AX4 ASH
Q6FJF3 CAN
C5DMP7 LAC
A7TM03 VAN
SIW14 YEAS Oca3
C5DPC1 ZYG
C4R2J9 PIC
A5DFC3 PIC
A5E1F7 LOD
B9WM87 CAN
Q59MU0 CAN
C4YMA3 CAN
C5M3N9 CAN
C4Y8A9 CLA
A3LXV4 PIC
Q6BYC6 DEB
Oca 3
A4R4G3 MAG
B2W0Y6 PYR
Q0UTD5 PHA
B8N9Z8 ASP
Q4WNU6 ASP
A1CH10 ASP
Q0CLA3 ASP
Q3M5U8 ASP
C8V8R3 EME
C0SIP8 PAR
C5GE36 AJE
C6H851 AJE
A5R7J2 AJE
C0NIT0 AJE
Oca-like
A8QCJ0 MAL
A2DLW1 TRI
D0MYB6 PHY
Q54MS1 DIC
D3BQ71 POL
Q38EE0 9TR
A4H3Z4 LEI
A4HS81 LEI
Q9U0Z9 LEI
C4QVQ0 PIC
Q6CEQ2 YAR
Q6CN54 KLU
Q754R3 ASH
C5E2U2 LAC
C5DZS6 ZYG
OCA6 YEAST
Q6FT58 CAN
A5E221 LOD
A5DB38 PIC
A3LWQ2 PIC
C4YBU3 CLA
Q6BK49 DEB
Q59ZY5 CAN
B9WA16 CAN
C5MC82 CAN
Oca 6
A5DEZ3 PIC
Q6BLU2 DEB
C4Y4S8 CLA
A3LQ98 PIC
A5DTK5 LOD
Q5A3M3 CAN
B9W9L1 CAN
C5MBJ2 CAN
C5DC41 LAC
Q6FVN9 CAN
OCA4 YEAST
C5DWU3 ZYG
A7TFY1 VAN
Q6CSQ2 KLU
Q75DA7 ASH
C4R595 PIC
Oca 4
Q54VX9 DIC
D1060 DICD
D3AZX6 POL
OCA1 USTMA
A2FYK3 TRI
Q55Y90 CRY
OCA1 YARLI
C4R237 PIC
OCA1 PICST
C5M588 CAN
C4YKT2 CAN
C4Y9S9 CLA
OCA1 DEBHA
OCA1 PICGU
OCA1 KLULA
C5DGX1 LAC
OCA1 ASHGO
A7TN95 VAN
C5DRL7 ZYG
OCA1 YEAST
Oca 1
C4R1Z1 PIC
Q6C7R1 YAR
B9WCJ4 CAN
C4YKJ6 CAN
C5M7D8 CAN
Q6BXK6 DEB
A5DGX3 PIC
C4Y837 CLA
A3LU65 PIC
C5DMK1 LAC
Q6CLF1 KLU
Q75B27 ASH
Q6FNP5 CAN
OCA2 YEAST
A7TLX6 VAN
C5DPA2 ZYG
Oca 2

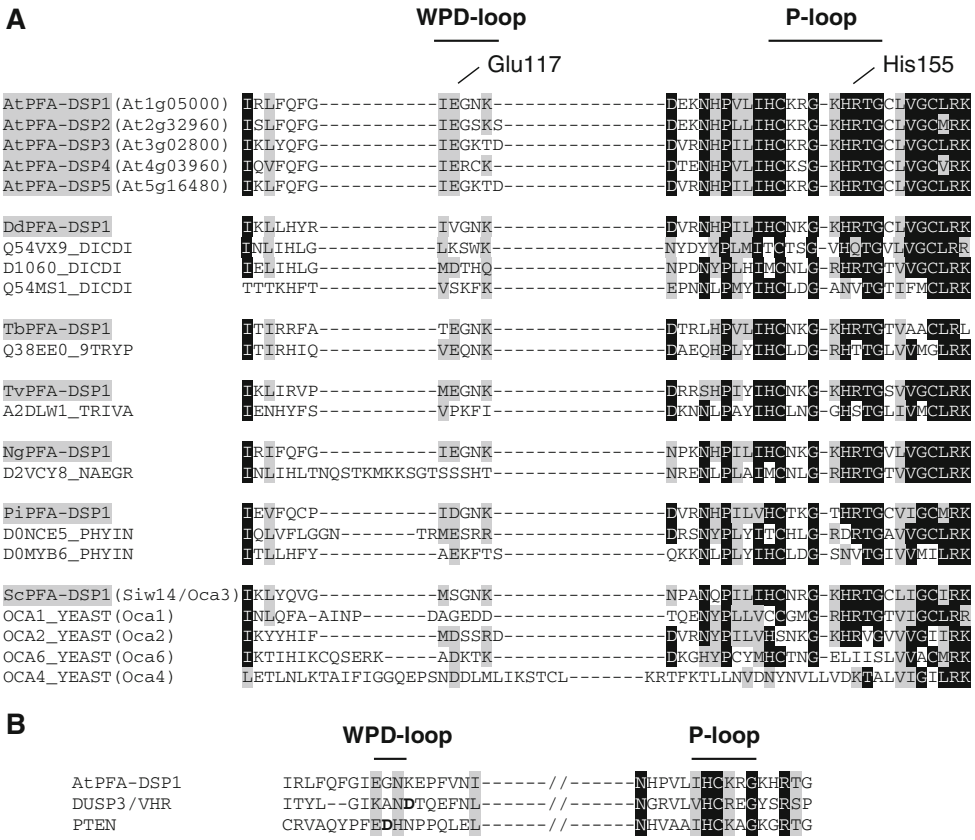

Fig. 2 Catalytic site comparison of PFA-DSPs and related proteins. Amino acid sequence alignment of the WPD-loop and the P-loop signature motif of PFA-DSPs (highlighted in *gray*) and PFA-DSP-related proteins from *A. thaliana* (At), *D. discoideum* (Dd), *T. brucei* (Tb), *T. vaginalis* (Tv), *N. gruberi* (Ng), *P. infestans* (Pi), and *S. cerevisiae* (Sc) (upper alignment). Residues Glu117 and His155 from AtPFA-DSP1/At1g05000 are indicated. The WPD- and P-loops for the distinct proteins were assigned from the AtPFA-DSP1 3D structure and alignment with the rest of sequences thereof. The lower alignment shows a comparison of the WPD-loop and P-loop of AtPFA-DSP1 and the mammalian DSPs DUSP3/VHR and PTEN. The catalytic Asp residues in the WPD-loop of DUSP3/VHR and PTEN are shown in *bold*. Identities are represented by *black boxes* and similarities by *gray boxes*

Leishmania), phylum Metamonada (*Trichomonas vaginalis*), phylum Percolozoa (*Naegleria gruberi*)], and the supergroup of Amoebozoa (*D. discoideum* and *Polysphondylium pallidum*). Finally, some PFA-DSP-related sequences belonged to the kingdom Chromista (*Phytophthora infestans*) (Figs. 1, 2; and Supplementary Table 1). Although all of the protein sequences are represented in fungi species, we could not identify Oca1 orthologs in fully sequenced genomes from Euglenozoa or Metamonada. Also, Oca2 is restricted to fungi species. On the other hand, Siw14/Oca3 and Oca6 putative orthologs can be found in all the aforementioned taxa (with the exception of *N. gruberi*, which did not display Oca6 ortholog). In some parasite kinetoplastid species (*T. brucei*, *L. major*), the orthologs of Siw14/Oca3 and Oca6 had been previously annotated as lipid-like or atypical DSPs, respectively (Brenchley et al. 2007). Given the high bootstrap support for the majority of the nodes clustering PFA-DSPs or PFA-DSP-related proteins and non-annotated proteins, it is likely that the absence of some orthologs is due to gene losses in particular taxa. This outlines the wide diversity of PFA-DSP-related genes in other kingdoms besides plants and fungi. Further BLASTP searches limited to specific eukaryotic taxa confirmed their absence in green algae, metazoans, or evolutionarily related organisms such as cnidarians or choanoflagellates. Also, PFA-DSP-related sequences were absent in bacteria species. A complete list of PFA-DSP and PFA-DSP-related sequences is given in Supplementary Table 1.

Molecular properties of PFA-DSPs

The PTP active site signature motif for PTPs (CX_5R; P-loop) is conserved in the majority of PFA-DSP and PFA-DSP-related proteins, although the catalytic Cys or Arg are absent in a few cases, including Oca2 and Oca6 in *S. cerevisiae*. In addition, Oca4 displays a different sequence at its catalytic loop that is likely to impair catalysis (Fig. 2), in line with the exclusion of Oca4 from the initial set of PFA-DSP-related sequences. This suggests that most of PFA-DSP and related proteins may be active enzymes and that non-catalytic proteins may also exist (see below). The P-loop sequences from PFA-DSP and PFA-DSP-related proteins are rich in basic residues (Lys and Arg), although variations exist that may be relevant to differences in catalysis and/or substrate specificity. Interestingly, most of the proteins lacking the essential Cys and/or Arg catalytic residues also lack basic residues at the P-loop, suggesting a functional divergence toward non-catalytic functions. The other catalytically relevant feature of PTPs, the WPD-loop, is particularly different in PFA-DSP and PFA-DSP-related proteins from distinct species (Fig 2). Some sequences

(including AtPFA-DSPs and kinetoplastid-PFA-DSPs) display a glutamic acid instead of the conserved aspartic acid (Denu et al. 1995) at the WPD-loop, and we have found that this glutamic acid residue does not serve in AtPFA-DSP1 (Glu117) as the putative general acid/base in catalysis (Romá-Mateo et al. 2007). In other sequences (including the *S. cerevisiae* Siw14/Oca3 or the *D. discoideum* DdPFA-DSP1 proteins), there are no negatively charged residues at this region. These observations strengthen the possibility that the catalysis of PFA-DSPs differs from the acid/base catalysis of classical PTPs (see below).

Next, we created 3D models of representative members of PFA-DSPs and PFA-DSP-related proteins from each taxon, using the available structural data of AtPFA-DSP1/At1g05000 (Aceti et al. 2008). Our modeling analysis revealed that the predicted surface charge distribution was well conserved, with a highly positive charge patch surrounding the active site cleft area in all cases (Fig 3a–c), in accordance with the enrichment in basic residues in the P-loop of these enzymes. It is interesting that another positive charge patch is present in the models corresponding to species from protozoan organisms, Amoebozoa and Chromista (Fig. 3b), which is absent in the models obtained from plants and fungi (Fig. 3a, c). This patch is located in the N-terminal portion of the protein and may serve as a functionally relevant area specific for those organisms. In addition, the *S. cerevisiae* Oca6 model displays a more elongated shape. Also of interest, the surface models of all PFA-DSP-related proteins in *S. cerevisiae*, although conserving a high positive charge of the active site cleft, show a preponderance of negatively charged residues that is not observed in the other PFA-DSPs (Fig. 3c).

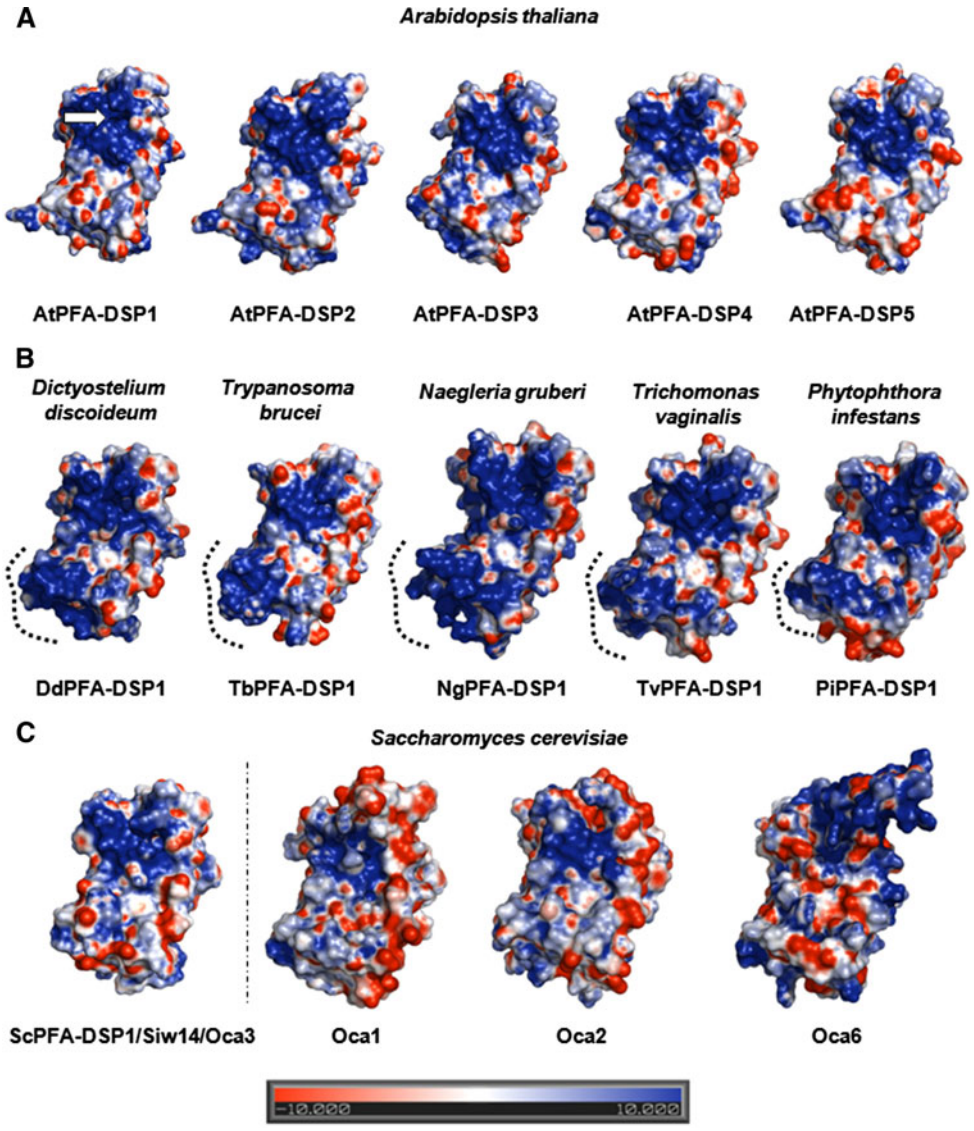

Fig. 3 Structure comparison of PFA-DSPs and related proteins from different taxa. **a** Structural models of PFA-DSPs from *A. thaliana*. The *arrow* in AtPFA-DSP1 indicates the positive charge patch surrounding the active site, which is present in all the models. Positive and negative charge potentials are in *blue* and *red*, respectively. **b** Structural models of PFA-DSPs from *D. discoideum, T. brucei*, *T. vaginalis*, *N. gruberi*, and *P. infestans.* The additional positive charge patches outside the catalytic pocket in protozoan species are indicated by *dotted lines*. **c** Structural models of PFA-DSP (*left*) and related proteins (*right*) from *S. cerevisiae*. Note the elongated shape displayed by Oca6. All models were created with the EsyPred3D server (Lambert et al. 2002) using the structure of AtPFA-DSP1 (PDB:1XRI) as template, and electrostatic potentials were created with a PyMOL APBS plug-in (Baker et al. 2001). Sequence identity values ranged from 50 to 60% between the model and Siw14/Oca3 or protozoan species, and from 21 to 26% between the model and PFA-related proteins

Expression, catalytic activity and substrate specificity of PFA-DSPs

PFA-DSPs from *A. thaliana* show a high degree of amino acid sequence identity (Figs. 1, 2); however, some of them display differential catalytic activity when tested for artificial phosphatase substrates (Romá-Mateo et al. 2007). To obtain a comprehensive and more physiological view of this group of proteins, we analyzed their distribution and expression levels in the plant. First, we analyzed the expression of the five *A. thaliana* PFA-DSP genes by semi-quantitative PCR and all of them were detected in several adult tissues (including root, stem, leaf, flower, and silique), although with a distinct expression pattern (Fig. 4a). To compare quantitatively the tissue expression patterns of the *A. thaliana* PFA-DSPs, their mRNA levels from the distinct tissues were quantified by quantitative real-time PCR (qrt-PCR) (Fig. 4b). Since the expression level of AtPFA-DSP2 was constant in all the tissues examined, we used AtPFA-DSP2 mRNA levels as a reference for data normalization. All the genes were detected in the studied tissues, although significant differences in the expression patterns were found, suggesting tissue-specific functions for these phosphatases. In general, the observed expression patterns were in agreement with the microarray data deposited in public databases (Zimmermann et al. 2004). These differences, together with the distinct PTP activity found for PFA-DSPs (see below), point to a functional diversity among members of PFA-DSPs.

The identification of the general acid/base moiety in the catalysis of AtPFA-DSP1 is relevant to ascertain the identity of the physiological substrates of AtPFA-DSP1 and related DSPs. Our previous studies ruled out the possibility that the glutamic acid at the WPD-loop in AtPFA-DSP1 (Glu117; Figs. 2, 4c) played the role of catalytic aspartic acid. In addition, the Asp191 residue, which is close to the catalytic cysteine (Cys150; Fig. 4c), was also disregarded as a catalytic residue (Romá-Mateo et al. 2007). The His155 residue at the P-loop of AtPFA-DSP1 is located at about 7A of the catalytic Cys150, making His155 a well-positioned residue to act as a proton donor in the hydrolysis reaction (Fig. 4c). Thus, His155 from AtPFA-DSP1 was mutated to glycine or to serine, which are the equivalent positioned residues in mammalian PTEN and VHR/DUSP3, respectively, and the catalytic activity of the mutations (H155G and H155S) was tested. The activity of AtPFA-DSP1 toward the phosphoinositides PI(3,4)P2 or PI(3,4,5)P3 was abrogated on the mutations H155G and H155S. However, both mutations displayed significant activity, although diminished in comparison with the wild type, toward the substrates OMFP and pNPP (Fig. 4c), indicating that the role of His155 in catalysis appears to be substrate dependent. It is likely that His155 from AtPFA-DSP1 participates in substrate recognition. These observations, together with our previous findings, suggest the absence of a canonical catalytic general acid/base residue in the active center of AtPFA-DSP1.

AtPFA-DSP1 dephosphorylates in vitro artificial PTP substrates, polyphosphates, Tyr-phosphorylated peptides, and phosphoinositides (Romá-Mateo et al. 2007; Aceti et al. 2008). The conservation of a positively charged active site cleft in PFA-DSPs prompted us to examine comparatively the substrate specificity of several AtPFA-DSPs and *S. cerevisiae* Siw14/Oca3. In vitro phosphatase assays were performed toward acidic substrates, such as the phosphoinositide PI(3,5)P2, as well as toward pTyr, OMFP, and pNPP (Fig. 4d). Interestingly, we found significant differences in phosphatase activity and substrate specificity not only between *A. thaliana* and *S. cerevisiae* proteins, but also between the distinct AtPFA-DSPs. All AtPFA-DSPs tested (AtPFA-DSP1, -2, -3, and -5) displayed phosphatase activity toward PI(3,5)P2, with AtPFA-DSP2 showing a higher activity. On using pTyr as the substrate, a distinct pattern of activity was found. AtPFA-DSP3 displayed higher activity toward pTyr; AtPFA-DSP1 and AtPFA-DSP2 showed a similar level of activity; and AtPFA-DSP5 was inactive toward this substrate, in contrast with the level of activity registered toward PI(3,5)P2. Noticeably, Siw14/Oca3 was inactive toward both PI(3,5)P2 and pTyr substrates. The lack of activity of AtPFA-DSP1 C150S catalytically inactive mutation is also shown (Fig. 4d). We also compared the activity of this set of enzymes toward the PTP artificial substrates OMFP and pNPP (Fig. 4d). The relative catalytic efficiencies of the phosphatases were similar for both substrates, with higher activity being displayed by AtPFA-DSP2, followed by AtPFA-DSP3. In contrast to the phosphatase assays using PI(3,5)P2 or pTyr as the substrates, Siw14/Oca3 was more active against OMFP and pNPP than AtPFA-DSP5, which displayed lower activity. The catalytic constants for all these proteins, using pNPP as the substrate and expressed as Kcat/Km (s^{-1} M^{-1}), are as follows: AtPFA-DSP1, 561.2; AtPFA-DSP2, 177.2; AtPFA-DSP3, 42.3; AtPFA-DSP5, 1.3; and Siw14/Oca3, 10.6 [(Romá-Mateo et al. 2007), and this report]. All enzymes were inactive to dephosphorylate pNPP in the presence of the PTP inhibitor sodium orthovanadate (data not shown). Together, these results indicate that the distinct PFA-DSPs exhibit different substrate specificities in vitro.

Genetic linkage among Oca proteins in yeast

The deletion of *OCA* genes in *S. cerevisiae* has been reported to confer sensitivity to some stresses (Rieger et al. 1999; Sakumoto et al. 2002; Care et al. 2004; Parsons et al. 2004; Dudley et al. 2005; Xie et al. 2005), in particular to

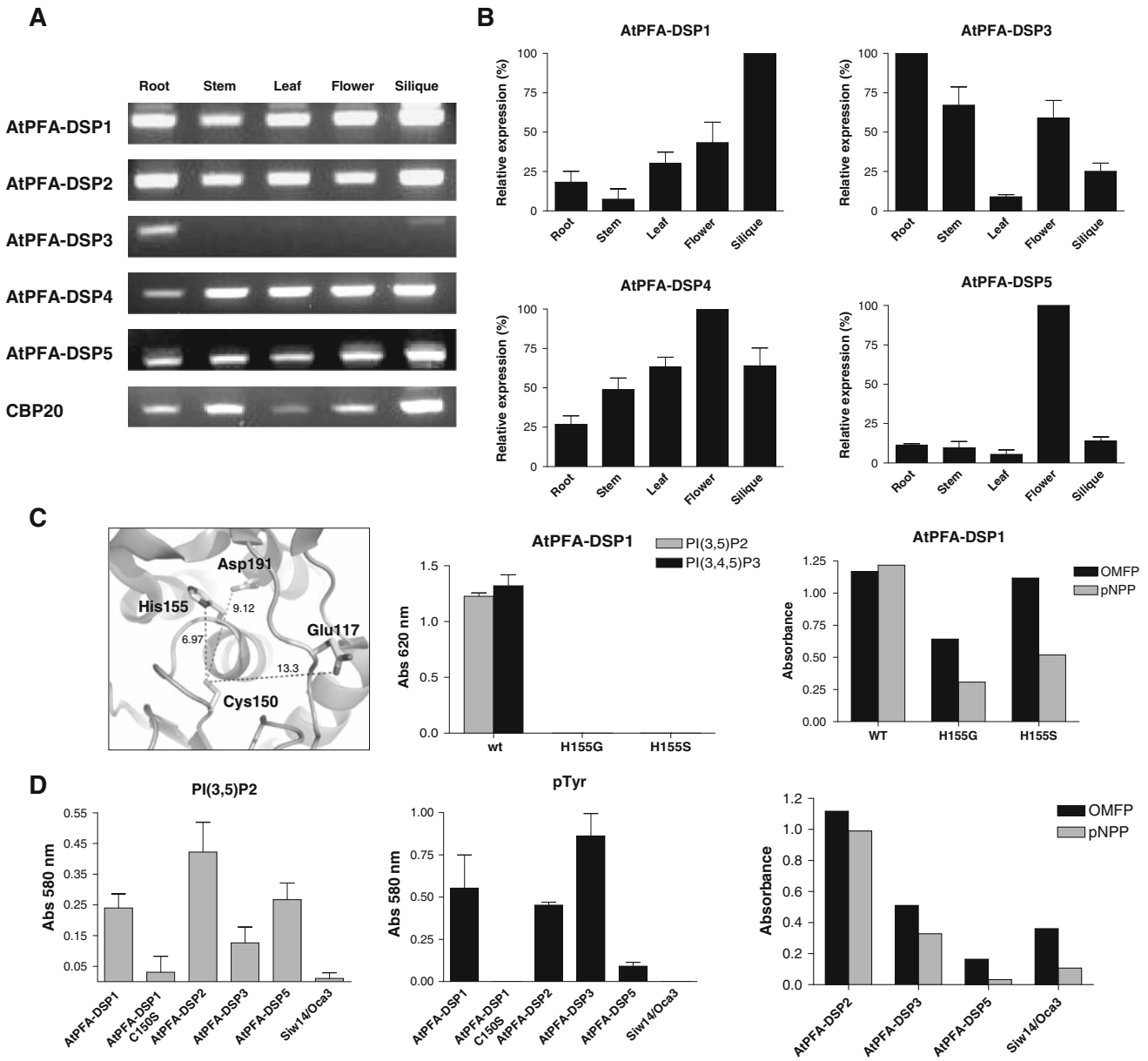

Fig. 4 Expression and catalytic activity of PFA-DSPs. **a** mRNA expression analysis using semiquantitative RT-PCR. Total RNA samples from different *A. thaliana* adult plant tissues were amplified by one-step RT-PCR using specific primers for each of the five AtPFA-DSP genes, and amplified DNA was resolved on agarose gels. The expression of the mRNA of the housekeeping gene CBP20 is also shown. **b** Tissue expression pattern of PFA-DSPs from *Arabidopsis thaliana*. Total RNA samples from different *A. thaliana* adult plant tissues were reverse transcribed to cDNA and used for qrt-PCR using primers specific for each AtPFA-DSP. Relative abundance of AtPFA-DSP genes in different *Arabidopsis* adult tissues is shown, normalized with respect to AtPFA-DSP2, the gene expression of which remained constant in all the analyzed tissues (CBP20 housekeeping displayed variations between tissues; see **a**). **c** Mutation of His155 in AtPFA-DSP1 does not abrogate its catalytic activity. Ribbon diagram detail of AtPFA-DSP1 catalytic site (*left panel*). The diagram shows the estimated distance between the catalytic cysteine (Cys150) and the WPD-loop acid residue Glu117 (13.3 A), as well as the distance to other putative proton donor/acceptor residues (Asp191 [9.12 A] and His155 [6.97 A]). Distances were calculated using PyMOL. Catalytic activity of His155 mutants (*middle panel*). In vitro phosphatase assays using 5 μg of purified GST fusion proteins and diC8-PI(3,5)P2 or diC8-PI(3,4,5)P2 as the substrates. Phosphate release was measured, after 45 min of reaction, as absorbance at 620 nm by the malachite green system. His155 was mutated to glycine (H155G) or to serine (H155S), mimicking the residues found in PTEN and DUSP3/VHR, respectively (see alignment in Fig. 2b). Both mutants were unable to dephosphorylate these substrates. In vitro phosphatase assays using 10 μg of purified GST fusion proteins (wild-type and His155 mutations) and pNPP or OMFP as the substrates (*right panel*). None of the mutations abrogated the catalytic activity of the enzyme toward these substrates. **d** PFA-DSPs phosphatase activity toward PI(3,5)P2, phospho-tyrosine (pTyr) and artificial PTP substrates (OMFP, pNPP). Reactions were carried out using 10 μg of purified GST fusion protein and diC8-PI(3,5)P2, phospho-tyrosine, OMFP or pNPP as the substrates. Phosphate release was measured during 100 min as absorbance at 580 nm by the malachite green system or as absorbance at either 490 nm (OMFP) or 405 nm (pNPP)

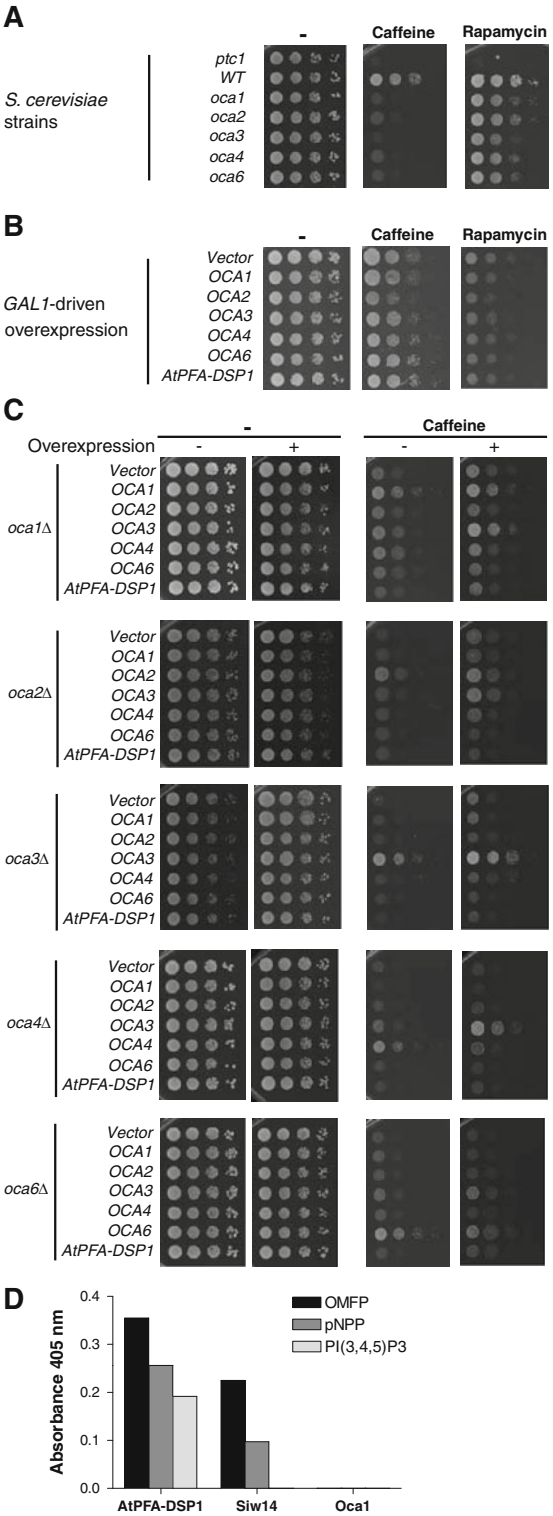

Fig. 5 Genetic linkage between Siw14/Oca3 and other Oca proteins. ▶ **a** Sensitivity to caffeine and rapamycin of the BY4741 (WT) and the isogenic mutant strains Y03702 (*ptc1Δ*), Y07235 (*oca1Δ*), Y07211 (*oca2Δ*), Y05358 (*oca3Δ*), Y06962 (*oca4Δ*), and Y04002 (*oca6Δ*). Cells were grown in liquid YPD medium at 30°C and a tenfold dilution series of this culture was spotted onto YPD agar media in the absence or presence of caffeine (10 mM), or rapamycin (5 ng/ml), and incubated for 3 days at 30°C. **b** Sensitivity to caffeine and rapamycin of cells overexpressing the indicated genes. Wild-type BY4741 cells were transformed with the multicopy pYES2 plasmid (vector), pYES2-AtPFA-DSP1, or the corresponding BG1805-based plasmid to overexpress the indicated *OCA* gene. Cells were grown in SD Ura-medium at 30°C and a tenfold dilution series of this culture were spotted onto YPG agar media, containing galactose as a carbon source, in the absence or presence of caffeine (14 mM), or rapamycin (10 ng/ml) and incubated for 3 days at 30°C. For better observation of the phenotype in the wild-type strain, higher concentrations of both compounds than in **a** were used in this experiment. **c** Complementation of the caffeine sensitivity of the distinct yeast *ocaΔ* mutants. Wild-type BY4741 (WT) and the isogenic mutant strains Y07235 (*oca1Δ*), Y07211 (*oca2Δ*), Y05358 (*oca3Δ*), Y06962 (*oca4Δ*), and Y04002 (*oca6Δ*) were transformed with the plasmids indicated in (**b**). Cells were grown in SD Ura-medium at 30°C and a tenfold dilution series of this culture was plated onto YPD (glucose) or YPG (galactose) in the absence (*left panels*; 2 days of incubation) or presence of 10 mM caffeine (*right panels*; 3 days of incubation). **d** Oca1 phosphatase activity toward OMFP, pNPP, and PI(3,4,5)P3. The experiment was performed as in Fig. 4c. No phosphatase activity was registered for Oca1

compounds that act as mTOR inhibitors such as caffeine and rapamycin (Kuranda et al. 2006; Zhou et al. 2010). All *oca* mutants have been shown to be caffeine sensitive, although some discrepancies were found in the strength of the phenotypes in the different studies. In the case of rapamycin, however, sensitivity was only observed in some of these mutants. To clarify this issue and compare the impact of the lack of distinct Oca proteins on the sensitivity to these TOR inhibitors, the growth of isogenic single *ocaΔ* mutants was analyzed on solid media containing caffeine or rapamycin. As a control, we used a mutant strain lacking the PP2C phosphatase Ptc1, which is known to be hypersensitive to both compounds (Gonzalez et al. 2009). As observed in Fig. 5a, all *ocaΔ* mutants displayed a high sensitivity to caffeine, which was slightly lower to that observed in the *ptc1* mutant. In contrast, although all mutants showed sensitivity to rapamycin, as compared to the isogenic wild-type strain, this was weak and much less intense than in the case of the *ptc1* strain. These results suggest the involvement of the Oca proteins in the regulation of TOR function. The amount of Oca2 seems to be particularly relevant to growth in the presence of these TOR inhibitors, since *GAL1*-driven overexpression of *OCA2* negatively affects yeast cell growth in the presence of either caffeine or rapamycin (Fig. 5b).

Since *S. cerevisiae* provides a simple and powerful system to analyze functional gene linkage, we exploited the higher sensitivity to caffeine of *ocaΔ* mutants as compared to rapamycin to analyze the ability of the different *OCA* genes to functionally complement this phenotype, when overexpressed in cells lacking each particular Oca protein. As shown in Fig. 5c, transcriptional leakage from the *GAL1* promoter under repression conditions (glucose) was

sufficient for every gene to complement the caffeine sensitivity of the corresponding mutant. Interestingly, galactose-induced overexpression of Siw14/Oca3 was able to restore growth, to some extent, of all *oca* mutants in the presence of caffeine. This phenotypic suppression was particularly evident for *oca1Δ* and *oca4Δ* mutants (Fig. 5c). Therefore, in contrast to the other Oca proteins, Siw14/Oca3 is able to replace in a dose-dependent manner the function of any of the other members of this yeast protein family. As can be observed in Fig. 5c, no functional suppression of the caffeine sensitivity of any of the yeast *ocaΔ* mutants was found under overexpression of AtPFA-DSP1/At1g05000 from *A. thaliana*, indicating distinct functions for these plant and yeast proteins. These results suggest that Siw14/Oca3 is genetically linked with the different Oca-related stress signaling pathways in *S. cerevisiae*, either by sharing effectors and/or substrates or by regulating common components of these pathways.

Siw14/Oca3 was the only Oca protein complementing the phenotype of all individual *ocaΔ* strains. Thus, we tested the putative phosphatase activity of Oca1, a protein that has been related to the triggering of cell cycle arrest by oxidative stress caused by linoleic acid hydroperoxide (Alic et al. 2001), in comparison with that displayed by Siw14/Oca3 and AtPFA-DSP1/At1g05000. As shown in Fig. 5d, Oca1 did not display measurable activity in vitro toward three different substrates, including OMFP, pNPP, and PI(3,4,5)P2, suggesting that Oca1 either lacks catalytic activity or possesses a restricted substrate specificity.

Discussion

In non-metazoan organisms, some PTPs share structural and catalytic properties with mammalian DSPs, dephosphorylate both p-Ser/Thr and p-Tyr residues, and possess a consensus catalytic motif, which is different from the classical PTP consensus catalytic motif. In general, classical PTPs have a narrowed active site that accommodates well the p-Tyr substrates; whereas DSPs have a shallowed active site, which permits the access to p-Ser and p-Tyr residues, as well as to other phosphorylated moieties (Yuvaniyama et al. 1996; Lee et al. 1999). PFA-DSPs constitute a subgroup within the non-mammalian DSPs, which is represented in plants, fungi, kinetoplastids and slime molds. In the model plant *A. thaliana*, there are five PFA-DSPs (AtPFA-DSP1/At1g05000, AtPFA-DSP2/At2g32960, AtPFA-DSP3/At3g02800, AtPFA-DSP4/At4g03960, and AtPFA-DSP5/At5g16480), and a variable number of PFA-DSPs exist in other plant species, such as *Oryza sativa* or *Zea mays*. However, only one PFA-DSP [as defined by the fingerprint technique (Attwood and Findlay 1993)] is present in fungi, kinetoplastids, and the slime mold *Dyctiostelium discoideum* (Romá-Mateo et al. 2007). Here, we have described the existence of a family of proteins from a non-metazoan taxa with amino acid sequence similarity to PFA-DSPs, and which are exemplified by the *S. cerevisiae* Oca1, Oca2, and Oca6 proteins, and, at a lesser extent, by Oca4 protein. These proteins are evolutionarily related to the PFA-DSP Siw14/Oca3 *S. cerevisiae* protein, and can be clustered together with orthologs from other fungi and protozoa species. An additional Oca-like subfamily of proteins was identified in our study, which was absent in *S. cerevisiae* but present in several Euascomyta fungi species from the subphylum Pezizomycotina (genera *Aspergillus* and *Ajellomyces*, among others) (Fig. 1). Our biochemical and bioinformatic analysis indicates the existence of both phosphatase-active and -inactive enzymes within this group of proteins. For instance, the presence of amino acid alterations or divergence in the catalytic loops of Oca2, Oca4, and Oca6 predicts a complete lack of phosphatase activity. In addition, Oca1, which presents a canonical catalytic P-loop, did not show phosphatase activity in our in vitro phosphatase assays using three different artificial substrates, suggesting that Oca1 is also an inactive phosphatase. However, we cannot rule out the possibility that Oca1 needs specific posttranslational modifications or requirements for catalysis in the yeast to be an active phosphatase. In this regard, our mutational analysis of the prototypic AtPFA-DSP1 protein suggests a particular mechanism of reaction for this enzyme. It also indicates that Glu117 and His155 residues at the catalytic site do not behave as proton/donor acceptors, but rather may participate in substrate recognition (Romá-Mateo et al. 2007) (Fig. 4c), as proposed for His111 from *S. cerevisiae* Sdp1 phosphatase (Fox et al. 2007), for Lys164 from *M. tuberculosis* MptpB phosphatase (Beresford et al. 2007), or for Lys128 in PTEN (Lee et al. 1999). The possibility exists that the physiologic substrates of PFA-DSPs and related proteins can act as the proton donor/acceptors in the hydrolysis reaction, as it seems to occur with the mammalian DSP Cdc25 (Chen et al. 2000).

Both plants and yeasts have developed complex signal transduction pathways that respond to a wide variety of stress conditions and allow adaptation of these organisms to changes in the environment. According to a putative role of the PFA-DSPs and related proteins in stress signaling regulation, Oca proteins from *S. cerevisiae* are required for growth in the presence of caffeine (Parsons et al. 2004; Dudley et al. 2005, and our results), a pleiotropic stress compound that is related with signaling through several yeast pathways, including MAPK and TOR (Hampsey 1997; Kuranda et al. 2006; Reinke et al. 2006). In addition, deletion in *OCA* genes rescues the telomeric DNA damage checkpoint response elicited in temperature-sensitive *cdc13-1* mutants (Addinall et al. 2008), and a *siw14/oca3Δ*

strain displays sensitivity to hygromycin B (Hirasaki et al. 2010). The mutant *siw14/oca3Δ* was shown to display a deficient response to nutrient deprivation (Care et al. 2004), which is consistent with the caffeine sensitivity of this mutant, since this compound is known to induce a starvation response in yeast cells (Winter et al. 2008). Oca proteins have also been related with the response to the TOR inhibitor rapamycin, since deletion of some *OCA* genes, including *oca1*, *oca2*, and *oca6*, conferred sensitivity to this compound in a genome-wide study (Xie et al. 2005). However, in other studies, *OCA* deleted strains were not sensitive to rapamycin (Parsons et al. 2004; Dudley et al. 2005). This is in agreement with our analysis showing that rapamycin causes a moderate growth inhibition on *OCA* deleted strains. Our complementation results demonstrate a genetic linkage between Siw14/Oca3 and the rest of Oca proteins associated with the caffeine-sensitivity stress pathway in *S. cerevisiae*. The function of Siw14/Oca3 in the caffeine-sensitivity pathway has been related to the function of the nitrogen-uptake kinase Npr, by controlling the intracellular location of the transcription factor Gln3 (Hirasaki et al. 2008). Furthermore, the involvement of Siw14/Oca3 in this pathway seems to be independent of Siw14/Oca3 catalytic activity, suggesting physiologic functions for this protein independent of catalysis (Care et al. 2004). This would be in accordance with our results on the lack of detectable phosphatase activity for Oca1 in vitro and on the predicted lack of catalytic activity for Oca2, Oca4, and Oca6. Interestingly, some of these enzymes have additional Cys residues in the vicinity of the P-loop, which could account for intramolecular disulfide bridge formation with functional implications. The existence of inactive PTPs has been well documented in mammals. These inactive enzymes can interact with signaling proteins and are potential regulators of protein phosphorylation-regulated signaling pathways by heterodimerization with active counterpart PTPs (Wishart and Dixon 1998; Gross et al. 2002; Begley and Dixon 2005; Gingras et al. 2009; Torii 2009; Hinton et al. 2010). In fact, physical interaction among Oca proteins has been detected in high-throughput two hybrid and mass spectrometry approaches (Ito et al. 2001; Collins et al. 2007). Interestingly, the *A. thaliana* AtPFA-DSP1 may form dimers (Aceti et al. 2008), making possible that the PFA-DSPs and related proteins may form homo- or hetero-dimers with regulatory functional relevance. In conclusion, our findings outline the functional complexity, both at the molecular and cellular levels, of the atypical dual-specificity phosphatases in non-metazoan organisms, which seem to have diverged toward catalytic and non-catalytic functions. Our results suggest physiological linkages between PFA-DSPs and related proteins beyond their activity as phosphatases. The identification of Oca-like proteins in different taxa makes these proteins relevant for further studies on the divergent functional evolution of the PTP superfamily in non-metazoan organisms. In *S. cerevisiae*, the genetic linkage found between Siw14/Oca3 and the other Oca proteins may help in the elucidation of the physiological function of these proteins and that of their orthologs in other organisms, including protozoa parasites causing infectious diseases in humans.

Acknowledgments This work was supported in part by grants SAF2006-08319 from Ministerio de Educación y Ciencia, SAF2009-10226 from Ministerio de Ciencia e Innovación (Spain and Fondo Europeo de Desarrollo Regional, FEDER; Plan de estímulo a la economía y el empleo, Plan E), AP-117/08, ACOMP2009/363 and ACOMP2010/222 from Generalitat Valenciana (Spain) (to R.P.), G0701233 from Medical Research Council (U.K.) (to L.T.), BIO2007-67299 from Ministerio de Ciencia e Innovación (Spain) (to M.M.), and by European Union Research Training Network MRTN-CT-2006-035830. C. Romá-Mateo and A. Sacristán-Reviriego have been recipients of predoctoral fellowships from Ministerio de Educación y Ciencia (Spain). We thank Peter Sudbery and José Luis Revuelta for providing cDNAs, the Arabidopsis Biological Resource Center (USA; donors: SSP Consortium, Sakis Theologis, Joe Ecker) for providing plasmids, and Isabel Roglá and Charis Saville for expert technical assistance.

References

Aceti DJ et al (2008) Structural and functional characterization of a novel phosphatase from the *Arabidopsis thaliana* gene locus At1g05000. Proteins 73:241–253

Addinall SG et al (2008) A genomewide suppressor and enhancer analysis of cdc13–1 reveals varied cellular processes influencing telomere capping in *Saccharomyces cerevisiae*. Genetics 180:2251–2266

Alic N, Higgins VJ, Dawes IW (2001) Identification of a *Saccharomyces cerevisiae* gene that is required for G1 arrest in response to the lipid oxidation product linoleic acid hydroperoxide*. Mol Biol Cell 12:1801–1810

Alonso A, Rojas A, Godzik A, Mustelin T (2004a) The dual-specific protein tyrosine phosphatase family. In: Ariño J, Alexander DR (eds) Topics in current genetics: protein phosphatases. Springer, Berlin, pp 333–358

Alonso A, Sasin J, Bottini N, Friedberg I, Friedberg I, Osterman A, Godzik A, Hunter T, Dixon J, Mustelin T et al (2004b) Protein tyrosine phosphatases in the human genome. Cell 117:699–711

Andreeva AV, Kutuzov MA (2008) Protozoan protein tyrosine phosphatases. Int J Parasitol 38:1279–1295

Attwood TK, Findlay JB (1993) Design of a discriminating fingerprint for G-protein-coupled receptors. Protein Eng 6:167–176

Attwood TK, Findlay JB (1994) Fingerprinting G-protein-coupled receptors. Protein Eng 7:195–203

Baker NA, Sept D, Joseph S, Holst MJ, McCammon JA (2001) Electrostatics of nanosystems: application to microtubules and the ribosome. Proc Natl Acad Sci USA 98:10037–10041

Bartels S et al (2009) MAP kinase phosphatase1 and protein tyrosine phosphatase1 are repressors of salicylic acid synthesis and SNC1-mediated responses in Arabidopsis. Plant Cell 21:2884–2897

Begley MJ, Dixon JE (2005) The structure and regulation of myotubularin phosphatases. Curr Opin Struct Biol 15:614–620

Beresford N, Patel S, Armstrong J, Szoor B, Fordham-Skelton AP, Tabernero L (2007) MptpB, a virulence factor from *Mycobacterium tuberculosis*, exhibits triple-specificity phosphatase activity. Biochem J 406:13–18

Beresford NJ, Saville C, Bennett HJ, Roberts IS, Tabernero L (2010) A new family of phosphoinositide phosphatases in microorganisms: identification and biochemical analysis. BMC Genomics 11:457

Brenchley R et al (2007) The TriTryp phosphatome: analysis of the protein phosphatase catalytic domains. BMC Genomics 8:434

Care A et al (2004) A synthetic lethal screen identifies a role for the cortical actin patch/endocytosis complex in the response to nutrient deprivation in *Saccharomyces cerevisiae*. Genetics 166:707–719

Chen W, Wilborn M, Rudolph J (2000) Dual-specific Cdc25B phosphatase: in search of the catalytic acid. Biochemistry 39:10781–10789

Collins SR et al (2007) Toward a comprehensive atlas of the physical interactome of *Saccharomyces cerevisiae*. Mol Cell Proteomics 6:439–450

Denu JM, Zhou G, Guo Y, Dixon JE (1995) The catalytic role of aspartic acid-92 in a human dual-specific protein-tyrosine-phosphatase. Biochemistry 34:3396–3403

Doi K et al (1994) MSG5, a novel protein phosphatase promotes adaptation to pheromone response in *S. cerevisiae*. EMBO J 13:61–70

Dudley AM, Janse DM, Tanay A, Shamir R, Church GM (2005) A global view of pleiotropy and phenotypically derived gene function in yeast. Mol Syst Biol 1:2005 0001

Felsentein J (1989) PHYLIP—phylogeny inference package (Version 3.2). Cladistics 5:164–166

Flandez M, Cosano IC, Nombela C, Martin H, Molina M (2004) Reciprocal regulation between Slt2 MAPK and isoforms of Msg5 dual-specificity protein phosphatase modulates the yeast cell integrity pathway. J Biol Chem 279:11027–11034

Fox GC et al (2007) Redox-mediated substrate recognition by Sdp1 defines a new group of tyrosine phosphatases. Nature 447:487–492

Gingras MC et al (2009) HD-PTP is a catalytically inactive tyrosine phosphatase due to a conserved divergence in its phosphatase domain. PLoS One 4:e5105

Gonzalez A, Ruiz A, Casamayor A, Arino J (2009) Normal function of the yeast TOR pathway requires the type 2C protein phosphatase Ptc1. Mol Cell Biol 29:2876–2888

Gross S et al (2002) Multimerization of the protein-tyrosine phosphatase (PTP)-like insulin-dependent diabetes mellitus autoantigens IA-2 and IA-2beta with receptor PTPs (RPTPs) inhibition of RPTPalpha enzymatic activity. J Biol Chem 277: 48139–48145

Guindon S, Gascuel O (2003) A simple, fast, and accurate algorithm to estimate large phylogenies by maximum likelihood. Syst Biol 52:696–704

Hahn JS, Thiele DJ (2002) Regulation of the *Saccharomyces cerevisiae* Slt2 kinase pathway by the stress-inducible Sdp1 dual specificity phosphatase. J Biol Chem 277:21278–21284

Hampsey M (1997) A review of phenotypes in *Saccharomyces cerevisiae*. Yeast 13:1099–1133

Hinton SD, Myers MP, Roggero VR, Allison LA, Tonks NK (2010) The pseudophosphatase MK-STYX interacts with G3BP and decreases stress granule formation. Biochem J 427:349–357

Hirasaki M, Kaneko Y, Harashima S (2008) Protein phosphatase Siw14 controls intracellular localization of Gln3 in cooperation with Npr1 kinase in *Saccharomyces cerevisiae*. Gene 409:34–43

Hirasaki M et al (2010) Deciphering cellular functions of protein phosphatases by comparison of gene expression profiles in *Saccharomyces cerevisiae*. J Biosci Bioeng 109:433–441

Ito T, Chiba T, Ozawa R, Yoshida M, Hattori M, Sakaki Y (2001) A comprehensive two-hybrid analysis to explore the yeast protein interactome. Proc Natl Acad Sci USA 98:4569–4574

Kennelly PJ (2001) Protein phosphatases—a phylogenetic perspective. Chem Rev 101:2291–2312

Kuranda K, Leberre V, Sokol S, Palamarczyk G, Francois J (2006) Investigating the caffeine effects in the yeast *Saccharomyces cerevisiae* brings new insights into the connection between TOR, PKC and Ras/cAMP signalling pathways. Mol Microbiol 61:1147–1166

Lambert C, Leonard N, De Bolle X, Depiereux E (2002) ESyPred3D: prediction of proteins 3D structures. Bioinformatics 18:1250–1256

Lee JO et al (1999) Crystal structure of the PTEN tumor suppressor: implications for its phosphoinositide phosphatase activity and membrane association. Cell 99:323–334

Luan S (2003) Protein phosphatases in plants. Annu Rev Plant Biol 54:63–92

Maehama T, Taylor GS, Dixon JE (2001) PTEN and myotubularin: novel phosphoinositide phosphatases. Annu Rev Biochem 70:247–279

Martin H, Flandez M, Nombela C, Molina M (2005) Protein phosphatases in MAPK signalling: we keep learning from yeast. Mol Microbiol 58:6–16

Moorhead GB, De Wever V, Templeton G, Kerk D (2009) Evolution of protein phosphatases in plants and animals. Biochem J 417:401–409

Nordle AK, Rios P, Gaulton A, Pulido R, Attwood TK, Tabernero L (2007) Functional assignment of MAPK phosphatase domains. Proteins 69:19–31

Owens DM, Keyse SM (2007) Differential regulation of MAP kinase signalling by dual-specificity protein phosphatases. Oncogene 26:3203–3213

Page RD (1996) TreeView: an application to display phylogenetic trees on personal computers. Comput Appl Biosci 12:357–358

Parsons AB et al (2004) Integration of chemical-genetic and genetic interaction data links bioactive compounds to cellular target pathways. Nat Biotechnol 22:62–69

Pfaffl MW (2001) A new mathematical model for relative quantification in real-time RT-PCR. Nucleic Acids Res 29:e45

Pincus D, Letunic I, Bork P, Lim WA (2008) Evolution of the phospho-tyrosine signaling machinery in premetazoan lineages. Proc Natl Acad Sci USA 105:9680–9684

Reinke A, Chen JC, Aronova S, Powers T (2006) Caffeine targets TOR complex I and provides evidence for a regulatory link between the FRB and kinase domains of Tor1p. J Biol Chem 281:31616–31626

Rieger KJ, El-Alama M, Stein G, Bradshaw C, Slonimski PP, Maundrell K (1999) Chemotyping of yeast mutants using robotics. Yeast 15:973–986

Romá-Mateo C, Ríos P, Tabernero L, Attwood TK, Pulido R (2007) A novel phosphatase family, structurally related to dual-specificity phosphatases, that displays unique amino acid sequence and substrate specificity. J Mol Biol 374:899–909

Sakumoto N, Matsuoka I, Mukai Y, Ogawa N, Kaneko Y, Harashima S (2002) A series of double disruptants for protein phosphatase genes in *Saccharomyces cerevisiae* and their phenotypic analysis. Yeast 19:587–599

Torii S (2009) Expression and function of IA-2 family proteins, unique neuroendocrine-specific protein-tyrosine phosphatases. Endocr J 56:639–648

Ulm R, Revenkova E, di Sansebastiano GP, Bechtold N, Paszkowski J (2001) Mitogen-activated protein kinase phosphatase is required for genotoxic stress relief in Arabidopsis. Genes Dev 15:699–709

Ulm R et al (2002) Distinct regulation of salinity and genotoxic stress responses by Arabidopsis MAP kinase phosphatase 1. EMBO J 21:6483–6493

Wilkes JM, Doerig C (2008) The protein-phosphatome of the human malaria parasite *Plasmodium falciparum*. BMC Genomics 9:412

Winter G, Hazan R, Bakalinsky AT, Abeliovich H (2008) Caffeine induces macroautophagy and confers a cytocidal effect on food spoilage yeast in combination with benzoic acid. Autophagy 4:28–36

Wishart MJ, Dixon JE (1998) Gathering STYX: phosphatase-like form predicts functions for unique protein-interaction domains. Trends Biochem Sci 23:301–306

Xie MW et al (2005) Insights into TOR function and rapamycin response: chemical genomic profiling by using a high-density cell array method. Proc Natl Acad Sci USA 102:7215–7220

Yuvaniyama J, Denu JM, Dixon JE, Saper MA (1996) Crystal structure of the dual specificity protein phosphatase VHR. Science 272:1328–1331

Zhou H, Luo Y, Huang S (2010) Updates of mTOR inhibitors. Anticancer Agents Med Chem 10:571–581

Zimmermann P, Hirsch-Hoffmann M, Hennig L, Gruissem W (2004) GENEVESTIGATOR. Arabidopsis microarray database and analysis toolbox. Plant Physiol 136:2621–2632